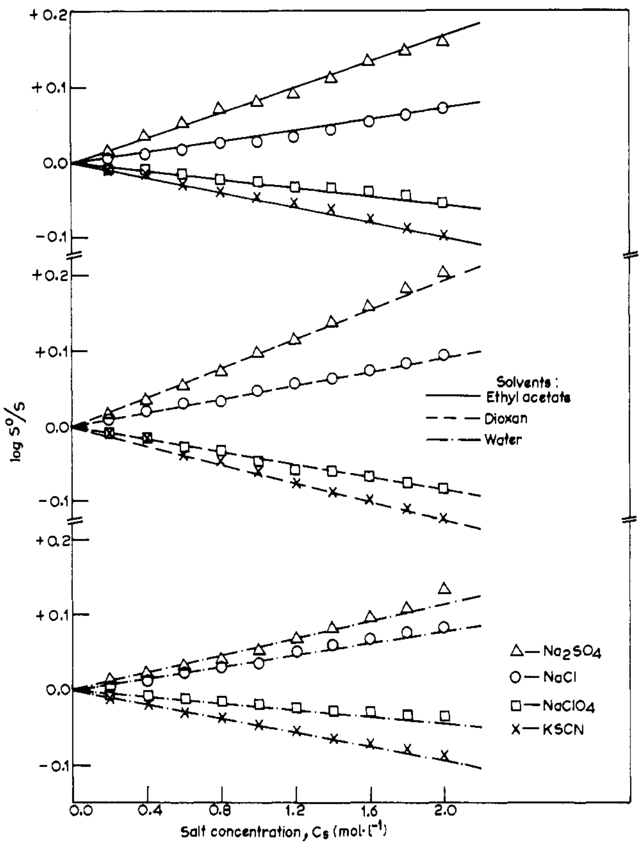

Figure 1. Solubility changes for *p*-aminophenol as a function of salt concentration.

creased. Hence, the free energy of the latter will rise; the largest change to be expected is that with the cation having the highest charge density. Apparently, the larger and more poorly hydrated ions have the opposite effect on the nonelectrolyte so that the free energy of the nonelectrolyte decreases and its solubility increases.

The salting out of PAP decreases in the order dioxane > ethyl acetate > water. This can be explained by considering that the ion-pair solvate in dioxane is more stabilized due to its low dielectric constant which precludes the solvation of the nonelectrolyte; hence, greater salting out is obtained. In ethyl acetate, due to the presence of two alkyl groups, the interaction with the aromatic part of PAP is greater and hence the salting out is less than in dioxane. In water, the salting out is even less and this can be explained by the stronger H bonding between water and PAP with acceptor sites. This effect predominates in spite of the greater solvation of the ions in water.

Registry No. PAP, 123-30-8; NaCl, 7647-14-5; Na_2SO_4, 7757-82-6; $NaClO_4$, 7601-89-0; KSCN, 333-20-0; ethyl acetate, 141-78-6; dioxane, 123-91-1.

Literature Cited

(1) McMeekin, T. L.; Cohn, E. J.; Weare, J. H. *J. Am. Chem. Soc.* **1936**, *58*, 2173-81.
(2) Cohn, E. J.; Edsal, J. "Proteins, Amino Acids and Peptides"; Reinhold: New York, 1943; p 200.
(3) Korenman, Ya. I.; Bortnikova, R. N. *Tr. Khim. Khim. Tekhnol.* **1974**, 127-8.
(4) Sado, E.; Kito, S.; Ito, Y. *J. Chem. Eng. Data* **1975**, *20*, 373-5.
(5) Yoshimura, Y.; Suzuki, N. *Talanta* **1978**, *25*, 489-91.
(6) Aquan-Yuen, M.; Mackay, D.; Shiu, W. Y. *J. Chem. Eng. Data* **1979**, *24*, 30-4.
(7) Ben-Naim, A.; Wilf, J. *J. Phys. Chem.* **1980**, *84*, 583-5.
(8) Setschenow, J. *Z. Phys. Chem.* **1889**, *4*, 117.
(9) Ghosh, R.; Das, B. *J. Indian Chem. Soc.* **1981**, *58*, 1108-10.

Received for review February 24, 1982. Revised manuscript received August 17, 1982. Accepted September 7, 1982.

Properties of $SOCl_2$-Based Electrolytes. 1. Conductivity, Viscosity, and Density

Hanumanthiya V. Venkatasetty*
Honeywell, Inc., Corporate Technology Center, Bloomington, Minnesota 55420

Stanislaw Szpak
Naval Ocean Systems Center, San Diego, California 92152

Specific conductivities, kinematic viscosities, and densities of $SOCl_2$–$AlCl_3$–LiCl electrolytes covering a wide range of compositions and temperatures were measured. A need for this information became evident when attempts were made to extend operational capabilities of highly energetic Li/$SOCl_2$ batteries to higher discharge rates. As we attempt to increase the rate of discharge, a new set of requirements must be met and new design concepts must be advanced to overcome ensuing difficulties. Most of these difficulties are traced to non-steady-state operation. Technical evaluations of any particular design can be made only if pertinent data are available.

In the past decade, new and highly energetic Li batteries have been developed (*1*). Among them, the Li/$SOCl_2$ system represents a new class of electrochemical energy conversion device—where the oxidant is at the same time solvent and depolarizer. The $SOCl_2$ molecules oxidize the metallic surface of the Li negative with the formation of a protective LiCl film and act as a solvent for Lewis acids, e.g., $AlCl_3$, thus providing ionic conductivity. They also function as a depolarizer yielding sulfur, sulfur dioxide, and chloride ions in the course of the cathodic process. Energy density of 600 W h kg^{-1}, in reserve, low rate configuration design, is routinely realized (*2*, *3*).

Recent efforts are directed toward the development and construction of cells capable of operation at high rates.

0021-9568/83/1728-0047$01.50/0

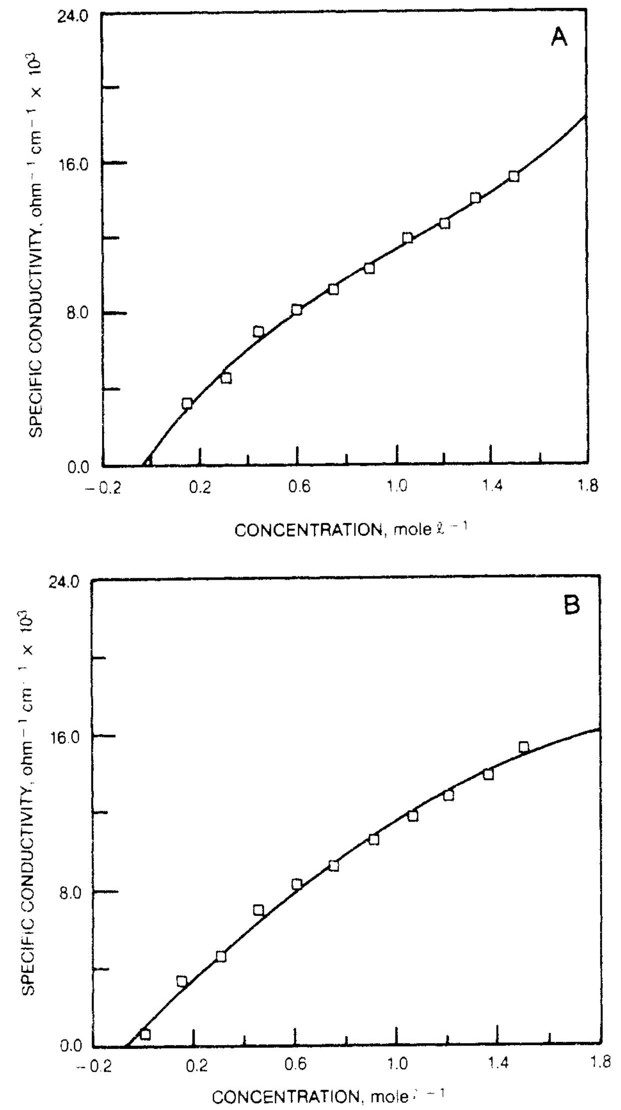

Figure 1. Specific conductivity of 1.5 M $AlCl_3$-$SOCl_2$ electrolyte as a function of LiCl concentration: (A) second-order polynomial fit; (B) third-order polynomial fit.

Steady-state current densities on the order of 75-85 mA cm^{-2} with short transient excursions in excess of 500 mA cm^{-2} have been obtained (*3*). However, as we attempt to increase the rate of discharge to its limit, the concept of a steady-state operation is no longer valid. Temperature and pressure continuously change, and concentration gradients and solution composition vary with time and location. New phases appear and the volume of electrolyte within the cell decreases with time. Indeed, a very complex situation develops created by various feedback mechanisms, which under adverse conditions may lead to catastrophic events. To avoid this, information concerning the behavior of battery functional elements must be assembled.

The purpose of this communication is twofold: first, to provide the needed data for the design and evaluation of high discharge rate Li/$SOCl_2$ batteries employing stationary and flowing electrolyte; second, to assemble experimental facts that are helpful in the discussion of structural characteristics of concentrated $SOCl_2$-based electrolytes which can be derived from measurements of their transport properties.

Presentation of Results

Experimental data were computer fitted to a polynomial

$$Y = A + Bx + Cx^2 + Dx^3 \qquad (1)$$

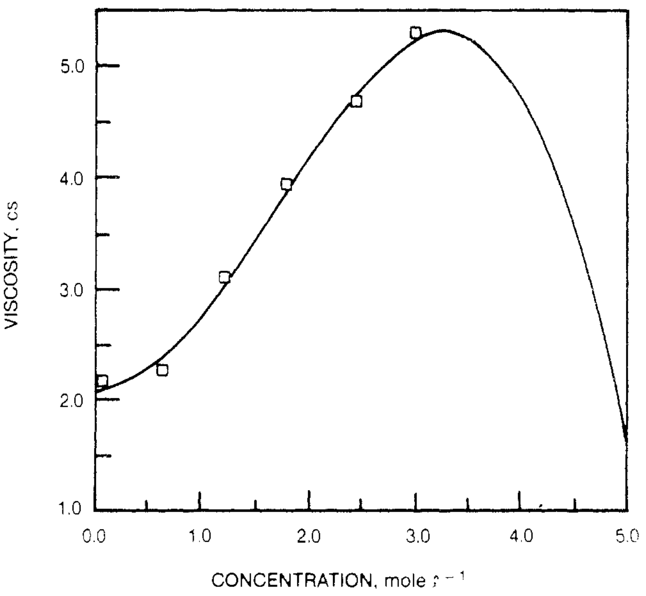

Figure 2. Kinematic viscosities of 3.0 M $AlCl_3$-$SOCl_2$ electrolyte as a function of LiCl concentration: third-order polynomial fit.

using the least-squares algorithm. The numerical values of coefficients A, B, ... are given in respective tables together with the correlation factor, CF, which represents the closeness of the fit. As an example, specific conductivities of the $SOCl_2$-1.5 M $AlCl_3$ electrolyte as a function of LiCl concentration are plotted in Figure 1, A and B. Here the same experimental data were fitted to a second-order polynomial

$$10^3Y = 1.0304 + 13.0712x - 2.5471x^2$$

with the CF = 0.998 (Figure 1A) and to a third-order polynomial

$$10^3Y = 0.6796 + 16.7869x - 9.043x^2 + 2.8871x^3$$

with the CF = 0.999 (Figure 1B). Evidently, specific conductivity for this case can be somewhat better represented by the third-order polynomial (note that CF = 1.000 is the perfect fit). A word of caution: Extrapolation beyond the ranges indicated in the tables should not be attempted, especially when using higher-order polynomials. This is illustrated in Figure 2 where the kinematic viscosities of the $SOCl_2$-3.0 M $AlCl_3$ as a function of LiCl concentration are represented by a third-order polynomial

$$Y = 2.10705 - 0.13969x + 0.9854x^2 - 0.1971x^3$$

with the CF = 0.999. If one wishes to extrapolate beyond the 3.0 M mark, one may be led to unreasonable conclusions. For convenience, all pertinent information is assembled in the same form. Thus, each table specifies electrolyte composition, experimental conditions, and applicable units of the property sought. The fixed part of the electrolyte composition is in parentheses and the variable part, that corresponding to the independent variable in eq 1, follows the parenthetical expression. The experimental conditions are listed in the first column of each table.

Specific Conductivities

The electrical conductance is the reciprocal of resistance which is derived from Ohm's law. The specific conductivity, σ, is given by eq 2, where R is the resistance in ohms, l is the

$$\sigma = R^{-1}(l/A) \qquad (2)$$

length in centimeters, and A is its cross-sectional area in cm^2. In conductivity cells, l and A are not directly measurable; however, their ratio needed in eq 2, the so-called cell constant,

Table I. Conductivity vs. Temperature for the Electrolyte $SOCl_2$-$AlCl_3$[a]

X_{AlCl_3}, M	A	B	C	D	CF
1.5	1.2441	9.1875×10^{-3}			0.998
	1.2431	9.4266×10^{-3}	-3.9849×10^{-6}		0.999
3.0	2.8434	0.02271	1.3626×10^{-4}		0.998
	2.8182	0.0181	4.0668×10^{-4}	-3.0045×10^{-6}	0.999
4.5	3.0154	0.0328	5.9905×10^{-4}		0.999
	3.0134	0.0324	6.2059×10^{-4}	-2.3939×10^{-6}	0.999

[a] Range: independent variable, $-10 < T < 70$ °C; experimental variable, $1.5 < X_{AlCl_3} < 4.5$ M. Units: Ω^{-1} cm^{-1} $\times 10^{-4}$.

Table II. Conductivity vs. LiCl Concentration for the Electrolyte $SOCl_2$-(1.5 M $AlCl_3$ + 0.5 M SO_2 + 0.15 M S)-X_{LiCl}[a]

T, °C	A	B	C	D	CF
−10	0.6483	11.5438	−2.046	0.5908	0.999
	0.5765	12.3042	−3.3757		0.999
0	1.0304	13.0712	−2.5471	2.8871	0.998
	0.6796	16.37869	−9.043		0.999
20	1.0517	15.6335	−2.8403	2.4829	0.998
	0.7500	18.829	8.4269		0.999
30	1.2563	16.3676	−2.7131	3.8375	0.998
	0.7901	21.3064	−11.3475		0.999
50	1.4799	17.6458	−2.6097	4.0924	0.998
	0.9826	22.9138	−11.8177		0.999
60	1.4691	17.0147	−2.0654	3.8512	0.998
	0.9826	21.9713	−10.7306		0.999
70	1.7084	17.2948	−2.2331	5.5584	0.997
	1.0064	24.6202	−14.8431		0.999

[a] Range: independent variable, $-0 < X_{LiCl} < 1.5$ M; experimental variable, $-10 < T < 70$ °C. Units: Ω^{-1} cm^{-1} $\times 10^{-3}$.

Table III. Conductivity vs. LiCl Concentration for the Electrolyte $SOCl_2$-(2.3 M $AlCl_3$)-X_{LiCl}[a]

T, °C	A	B	C	D	CF
0	2.0868	158.434	−81.3672	201.042	0.999
	1.6981	183.725	−229.993		0.999
40	4.6266	211.963	−106.351	328.743	0.999
	3.9910	253.318	−349.383		1.00
60	6.3265	227.314	−104.605	318.302	0.999
	5.7111	267.355	−339.919		1.00

[a] Range: independent variable, $0 < X_{LiCl} < 0.5$ M; experimental variable, $0 < T < 60$ °C. Units: Ω^{-1} cm^{-1} $\times 10^{-3}$.

Table IV. Conductivity vs. LiCl Concentration for the Electrolyte $SOCl_2$-(3 M $AlCl_3$ + 0.5 M SO_2 + 0.15 M S)-X_{LiCl}[a]

T, °C	A	B	C	D	CF
−10	1.2077	4.8048	−0.5845	0.3569	0.996
	0.8608	6.6423	−2.1907		0.999
0	1.4057	5.6643	−0.6004	0.4196	0.996
	0.9978	7.8243	−2.4885		0.999
10	1.6820	7.0900	−0.8768	0.5525	0.996
	1.1449	9.9344	−3.3631		0.999
20	1.7883	7.6931	−0.6518	0.5732	0.997
	1.2311	10.6439	−3.2311		0.999
30	2.0136	9.4095	−1.0991	0.7432	0.996
	1.2912	13.2356	−4.4436		0.999
40	2.2164	10.3338	−1.1247	0.7902	0.996
	1.4482	14.4021	−4.6808		0.999
50	2.4348	11.1569	−1.1225	0.8360	0.997
	1.6222	15.4604	−4.8844		0.999
60	2.6372	11.6938	−1.0141	0.6420	0.998
	2.0131	14.9988	−3.9031		0.999
70	2.8347	12.2643	−0.9195	0.6302	0.998
	2.2221	15.5088	−3.7555		0.999

[a] Range: independent variable, $0 < X_{LiCl} < 3.0$ M; experimental variable, $-10 < T < 70$ °C. Units: Ω^{-1} cm^{-1} $\times 10^{-3}$.

is determined experimentally by calibration with aqueous KCl solutions of known concentrations (*4*). The cell constant at temperatures other than 25 °C was computed by using the Washburn method (*5*).

Table V. Conductivity vs. LiCl Concentration for the Electrolyte $SOCl_2$-(4.5 M $AlCl_3$)-X_{LiCl}[a]

T, °C	A	B	C	D	CF
0	2.8633	70.601	−52.6211	93.5936	0.999
	2.7335	82.5361	−112.407		1.000
15	3.4339	84.6809	−44.704	−1.6546	1.000
	3.4371	84.4727	−43.4808		1.000
25	4.0748	111.78	−80.3792	191.98	0.999
	3.7037	135.931	−222.308		0.999
40	6.0248	131.048	−87.8522	−78.3686	0.999
	6.1763	121.189	−29.9159		1.000
60	8.5735	144.614	−72.0786	115.909	0.999
	8.3494	159.768	−157.768		1.000

[a] Range: independent variable, $0 < X_{LiCl} < 0.5$ M; experimental variable, $0 < T < 60$ °C. Units: Ω^{-1} cm^{-1} $\times 10^{-3}$.

Table VI. Conductivity vs. LiCl Concentration for the Electrolyte $SOCl_2$-(4.5 M $AlCl_3$ + 0.5 M SO_2 + 0.15 M S)-X_{LiCl}[a]

T, °C	A	B	C	D	CF
−10	0.9926	1.3529	−0.1013	0.1155	0.979
	0.6079	2.6963	−0.8799		0.998
0	1.020	2.1823	−0.2252	0.0981	0.988
	0.7318	3.2972	−0.8841		0.997
20	1.8418	3.1273	−0.1825	0.1788	0.991
	1.2460	5.2072	−1.3881		0.998
30	2.1457	3.8609	−0.2110	0.1879	0.993
	1.5197	6.0467	−1.4779		0.998
40	2.4227	4.6009	−0.2174	0.2091	0.995
	1.7368	7.0226	−1.6287		0.999
50	2.5955	5.7117	−0.3713	0.1590	0.997
	2.0740	7.5530	−1.4444		0.999
60	3.1029	6.0784	−0.2069	0.2122	0.997
	2.4067	8.5364	−1.6393		0.999
70	3.6433	6.7824	−0.1934	0.2291	0.998
	2.8137	9.4789	−1.746		0.999

[a] Range: independent variable, $0 < X_{LiCl} < 4.5$ M; experimental variable, $-10 < T < 70$ °C. Units: Ω^{-1} cm^{-1} $\times 10^{-3}$.

Table VII. Conductivity vs. SO_2 Concentration for the Electrolyte $SOCl_2$-(3 M $AlCl_3$ + 0.15 M S + 1.5 M LiCl)-X_{SO_2}[a]

T, °C	A	B	C	D	CF
10	99.3834	10.4483	1.7241	−0.5525	0.999
	99.4663	9.2604	3.3815		0.999
30	130.887	17.8253	0.8306	−0.3604	1.000
	130.941	17.0505	1.9118		1.000
50	159.919	22.3591	0.1809	−0.2734	1.000
	159.96	21.7713	1.0011		1.000

[a] Range: independent variable, $0 < X_{SO_2} < 2.0$ M; experimental variable, $10 < T < 50$ °C. Units: Ω^{-1} cm^{-1} $\times 10^{-3}$.

***Experimental Procedure*.** The basic apparatus for the determination of electrolytic conductance is a modified Wheatstone bridge which compensates for the capacitance during the balancing process. Here, the Jones and Josephs-type bridge (*6*), in combination with a Wavetek function generator and oscilloscope, was employed (*7*). Accuracies on the order of 1% are routinely obtained if the temperature is controlled to within ±0.5 °C.

***Results*.** Specific conductivities of $SOCl_2$-based electrolytes were determined as a function of concentration (X, M) and

Table VIII. Viscosity vs. Temperature for the Electrolyte $SOCl_2$-(1.5 M $AlCl_3$ + 0.5 M SO_2 + 0.15 M S)-X_{LiCl}[a]

X_{LiCl}, M	A	B	C	D	CF
0.15	0.9255	−0.012 73	8.8684×10^{-5}		0.999
	0.9263	−0.912 60	8.0716×10^{-5}	8.8528×10^{-8}	0.999
0.45	1.0780	−0.014 5	9.0943×10^{-5}		0.999
	1.0804	−0.014 0	6.5826×10^{-5}	2.7868×10^{-7}	0.999
0.60	1.0935	−0.014 61	9.3384×10^{-5}		0.999
	1.0945	−0.014 42	8.1869×10^{-5}	1.2794×10^{-7}	0.999
0.90	1.2116	−0.015 82	8.9865×10^{-5}		0.998
	1.2148	−0.015 26	5.6413×10^{-5}	3.7169×10^{-7}	0.998
1.2	1.3877	−0.017 90	9.9216×10^{-5}		0.997
	1.3912	−0.017 26	6.0886×10^{-5}	4.2590×10^{-7}	0.997
1.5	1.4679	−0.017 14	8.6149×10^{-5}		0.998
	1.4702	−0.016 71	6.1157×10^{-5}	2.7768×10^{-7}	0.998

[a] Range: independent variable, $-10 < T < 70$ °C; experimental variable, $0.15 \leqslant X_{LiCl} \leqslant 1.5$ M. Units: centistokes.

Table IX. Viscosity vs. Temperature for the Electrolyte $SOCl_2$-(3.0 M $AlCl_3$ + 0.5 M SO_2 + 0.15 M S)-X_{LiCl}[a]

X_{LiCl}, M	A	B	C	D	CF
0	1.8266	−0.030 33	2.1528×10^{-4}		0.997
	1.8244	−0.030 74	2.3959×10^{-4}	-2.7013×10^{-7}	0.997
0.6	1.9719	−0.932 23	2.2475×10^{-4}		0.998
	1.9757	−0.031 55	1.8435×10^{-4}	4.4891×10^{-7}	0.998
1.2	2.5706	−0.045 35	3.1824×10^{-4}		0.999
	2.5674	−0.045 92	3.5252×10^{-4}	-3.8087×10^{-7}	0.999
1.8	3.2270	−0.062 96	4.6101×10^{-4}		0.999
	3.2104	−0.065 96	6.3873×10^{-4}	-1.9746×10^{-6}	0.999
2.4	3.8266	−0.077 39	5.8094×10^{-4}		0.998
	3.8008	−0.082 05	8.5677×10^{-4}	-3.0647×10^{-6}	0.999
3.0	4.3380	−0.086 74	6.2817×10^{-4}		0.998
	4.3203	−0.089 95	8.1817×10^{-4}	-2.1111×10^{-6}	0.998

[a] Range: independent variable, $-10 < T < 70$ °C. Experimental variable, $0 < X_{LiCl} < 3.0$ M. Units: centistokes.

Table X. Viscosity vs. Temperature for the Electrolyte $SOCl_2$-(4.5 M $AlCl_3$ + 0.5 M SO_2 + 0.15 M S)-X_{LiCl}[a]

X_{LiCl}, M	A	B	C	D	CF
0	3.1764	−0.0674	5.0948×10^{-4}		0.982
	3.1456	−0.0730	8.3991×10^{-4}	-3.6714×10^{-6}	0.983
0.45	5.4757	−0.1101	7.3802×10^{-4}		0.999
	5.4913	−0.1072	5.6988×10^{-4}	1.8682×10^{-6}	0.999
0.90	6.7586	−0.1556	1.0322×10^{-3}		0.999
	6.7607	−0.1442	1.0096×10^{-3}	2.5107×10^{-7}	0.999
1.8	8.8325	−0.1993	1.4803×10^{-3}		0.998
	8.8524	−0.1957	1.2662×10^{-3}	2.3791×10^{-6}	0.998
2.7	9.6294	−0.2257	1.7414×10^{-3}		0.999
	9.6053	−0.2300	1.9991×10^{-3}	-2.8623×10^{-6}	0.999
3.60	11.5147	−0.2697	2.0919×10^{-3}		0.999
	11.4902	−0.2741	2.3537×10^{-3}	-2.9088×10^{-6}	0.998
4.5	13.256	−0.3036	2.2441×10^{-3}		0.999
	13.2574	−0.3034	2.2292×10^{-3}	1.6497×10^{-7}	0.999

[a] Range: independent variable, $-10 < T < 70$ °C; experimental variable, $0 < X_{LiCl} < 4.5$ M. Units: centistokes.

Table XI. Viscosity vs. LiCl Concentration for the Electrolyte $SOCl_2$-(1.5 M $AlCl_3$ + 0.5 M SO_2 + 0.15 M S)-X_{LiCl}[a]

T, °C	A	B	C	D	CF
−10	1.002	0.4242	5.1806×10^{-3}		0.994
	1.0105	0.3691	0.0881	−0.0339	0.994
0	0.8523	0.5027	−0.0472		0.988
	0.8985	0.2041	0.4019	−0.1836	0.990
10	0.7730	0.2830	0.0516		0.994
	0.7645	0.3380	−0.0311	0.0338	0.994
20	0.6498	0.3778	−0.0337		0.995
	0.6672	0.2658	0.1346	−0.0688	0.995
30	0.6390	0.0645	0.1407		0.990
	0.5718	0.4578	−0.4330	0.2337	0.997
40	0.5234	0.2282	0.0234		0.996
	0.5281	0.1925	0.0695	−0.0188	0.996
50	0.4993	0.1357	0.0492		0.992
	0.4734	0.2925	−0.1867	0.0972	0.994
60	0.4706	0.0894	0.0642		0.996
	0.4568	0.1781	0.0690	0.0545	0.997
70	0.4707	0.0331	0.0760		0.991
	0.4451	0.1984	−0.1725	0.1016	0.995

[a] Range: independent variable, $0 < X_{LiCl} < 1.5$ M; experimental variable, $-10 < T < 70$ °C. Units: centistokes.

Table XII. Viscosity vs. LiCl Concentration for the Electrolyte $SOCl_2$-(3.0 M $AlCl_3$ + 0.5 M SO_2 + 0.15 M S)-X_{LiCl}[a]

T, °C	A	B	C	D	CF
−10	1.9792	0.8327	0.0982		0.992
	2.1070	−0.1396	0.9854	−0.1971	0.999
0	1.8168	0.5069	0.1320		0.995
	1.8937	−0.0782	0.6659	−0.1186	0.999
10	1.4437	0.5303	0.0493		0.996
	1.4921	0.1620	0.3852	−0.0746	0.999
20	1.2275	0.4185	0.0336		0.995
	1.2680	0.1103	0.3148	−0.0624	0.998
30	1.0747	0.2530	0.0579		0.997
	1.0871	0.1587	0.1440	−0.0191	0.998
40	0.9550	0.2201	0.0322		0.996
	0.9757	0.0624	0.1761	−0.0319	0.999
50	0.8353	0.2101	0.0199		0.993
	0.8594	0.0272	0.1867	−0.0370	0.998
60	0.7666	0.1655	0.0182		0.998
	0.7782	0.0775	0.0985	−0.0178	0.999
70	0.7401	0.1493	0.0136		0.996
	0.7486	0.0848	0.0724	−0.0130	0.998

[a] Range: independent variable, $0 < X_{LiCl} < 3.0$ M; experimental variable, $-10 < T < 70$ °C. Units: centistokes.

Table XIII. Viscosity vs. LiCl Concentration for the Electrolyte $SOCl_2$-(4.5 M $AlCl_3$ + 0.5 M SO_2 + 0.15 M S)-X_{LiCl}[a]

T, °C	A	B	C	D	CF
−10	4.5407	3.8082	−0.2775		0.992
	3.9757	6.1293	−1.658	0.2035	0.998
0	3.9985	2.7640	−0.1642		0.992
	3.5517	4.5998	−1.2567	0.1610	0.998
10	2.9159	2.556	−0.2055		0.978
	2.3173	5.0147	−1.6691	0.2156	0.995
20	2.6230	1.5257	−0.0875		0.984
	2.2640	3.0007	−0.9653	0.1293	0.998
30	1.8534	1.3251	−0.1022		0.980
	1.5585	2.5367	−0.8233	0.1062	0.995
40	1.6686	0.89774	−0.0521		0.984
	1.4748	1.6942	−0.5261	0.0698	0.995
50	1.4217	0.6994	−0.0420		0.987
	1.2874	1.2508	−0.3702	0.0483	0.996
60	1.0982	0.6600	−0.9410		0.986
	0.9686	1.1924	−0.3578	0.0466	0.996
70	1.0111	0.7073	−0.0638		0.990
	0.9485	0.9648	−0.2170	0.0225	0.992

[a] Range: independent variable, $0 < X_{LiCl} < 4.5$ M; experimental variable, $-10 < T < 70$ °C. Units: centistokes.

temperature (T, °C). Results are summarized in Tables I–VII, where coefficients A, B, ... of the polynomial fit are given. The accuracy of representation, expressed by the correlation factor, CF, is included.

Viscosity

The concept of viscosity arises from the frictional resistance to shearing stress and is defined as the tangential force acting on unit area of one of the two parallel planes at unit distance apart, filled with liquid, and moving relative to each other with unit velocity. Kinematic viscosity, ν, rather than the absolute

Table XIV. Density vs. Temperature for the Solvent $SOCl_2$[a]

A	B	C	D	CF
1.6763	-1.8200×10^{-3}	-1.4988×10^{-7}		0.999
1.6763	-1.8324×10^{-3}	2.7142×10^{-7}	-3.1208×10^{-9}	0.999

[a] Range: experimental variable, $-10 < T < 100$ °C. Units: g cm^{-3}.

Table XV. Density vs. Temperature for the Electrolyte $SOCl_2$-X_{AlCl_3}[a]

X_{AlCl_3}, M	A	B	C	D	CF
1.5	1.7156	-1.7958×10^{-3}	6.5467×10^{-7}		0.999
	1.7155	-1.8137×10^{-3}	1.7445×10^{-6}	-1.2241×10^{-8}	0.999
3.0	1.7227	-1.6731×10^{-3}	3.0801×10^{-8}		0.999
	1.7227	-1.6795×10^{-3}	2.5489×10^{-7}	-1.6819×10^{-9}	0.999
4.5	1.7727	-1.6304×10^{-3}	2.1942×10^{-7}		0.999
	1.7727	-1.6603×10^{-3}	1.2573×10^{-6}	-7.7899×10^{-9}	0.999

[a] Range: independent variable, $-10 < T < 70$ °C; experimental variable, $1.5 < X_{AlCl_3} < 4.5$ M. Units: g cm^{-3}.

Table XVI. Density vs. Temperature for the Electrolyte $SOCl_2$-(1.5 M $AlCl_3$ + 0.5 M SO_2 + 0.15 M S)-X_{LiCl}[a]

X_{LiCl}, M	A	B	C	D	CF
0.15	1.7136	-1.8105×10^{-3}	1.2494×10^{-6}		0.998
	1.7147	-1.6860×10^{-3}	-4.6603×10^{-6}	5.6248×10^{-8}	0.999
0.45	1.7156	-1.6787×10^{-3}	-6.0621×10^{-7}		0.999
	1.7156	-1.6789×10^{-3}	-6.0027×10^{-7}	-4.9460×10^{-11}	0.999
0.6	1.7153	-1.6254×10^{-3}	-8.3898×10^{-7}		0.999
	1.7153	-1.5861×10^{-3}	-2.4510×10^{-6}	1.3752×10^{-8}	0.999
0.9	1.7192	-1.5605×10^{-3}	-1.5613×10^{-6}		0.999
	1.7195	-1.4194×10^{-3}	-7.1687×10^{-6}	4.6727×10^{-8}	0.999
1.2	1.7247	-1.5659×10^{-3}	-1.7917×10^{-7}		0.999
	1.7247	-1.5415×10^{-3}	-1.1793×10^{-6}	8.5188×10^{-9}	0.999
1.5	1.7260	-1.6776×10^{-3}	-2.9094×10^{-7}		0.999
	1.7261	-1.6432×10^{-3}	-1.6590×10^{-6}	1.1401×10^{-8}	0.999

[a] Range: independent variable, $-10 < T < 90$ °C; experimental variable, $0.15 < X_{LiCl} < 1.5$ M. Units: g cm^{-3}.

Table XVII. Density vs. Temperature for the Electrolyte $SOCl_2$-(3 M $AlCl_3$ + 0.5 M SO_2 + 0.15 M S)-X_{LiCl}[a]

X_{LiCl}, M	A	B	C	D	CF
0	1.7154	-1.4259×10^{-3}	1.4439×10^{-6}		0.997
	1.7151	-1.5253×10^{-3}	5.9841×10^{-6}	-4.2027×10^{-8}	0.997
0.3	1.7492	-1.8172×10^{-3}	2.1482×10^{-7}		0.999
	1.7493	-1.7711×10^{-3}	-1.3600×10^{-6}	1.1665×10^{-8}	0.999
0.6	1.7433	-1.6078×10^{-3}	2.7997×10^{-7}		0.999
	1.7431	-1.6808×10^{-3}	3.1812×10^{-6}	-2.4177×10^{-8}	0.999
1.2	1.7474	-1.5524×10^{-3}	-1.1658×10^{-7}		0.999
	1.7475	-1.5485×10^{-3}	-2.7337×10^{-7}	1.3065×10^{-9}	0.999
1.8	1.7455	-1.6076×10^{-3}	-2.4255×10^{-8}		0.999
	1.7456	-1.5996×10^{-3}	-2.9687×10^{-7}	2.0193×10^{-9}	0.999
2.4	1.7480	-1.4595×10^{-3}	-2.2142×10^{-7}		0.999
	1.7479	-1.5036×10^{-3}	1.5283×10^{-6}	-1.4581×10^{-8}	0.999
3.0	1.6908	-1.5667×10^{-3}	-1.7135×10^{-6}		0.999
	1.691	-1.4346×10^{-3}	-6.2279×10^{-6}	3.3439×10^{-8}	0.999

[a] Range: independent variable, $-10 < T < 100$ °C; experimental variable, $0 < X_{LiCl} < 3.0$ M. Units: g cm^{-3}.

Table XVIII. Density vs. Temperature for the Electrolyte $SOCl_2$-(4.5 M $AlCl_3$ + 0.5 M SO_2 + 0.15 M S)-X_{LiCl}[a]

X_{LiCl}, M	A	B	C	D	CF
0	1.7735	-1.6817×10^{-3}	9.0864×10^{-7}		0.999
	1.7736	-1.6274×10^{-3}	-9.4880×10^{-7}	1.3758×10^{-8}	0.999
0.45	1.7580	-1.2880×10^{-3}	-3.6258×10^{-7}		0.999
	1.7580	-1.2842×10^{-3}	-4.8975×10^{-7}	9.4201×10^{-10}	0.999
0.9	1.7662	-1.4073×10^{-3}	-7.3602×10^{-7}		0.994
	1.7665	-1.1458×10^{-3}	-9.7032×10^{-6}	6.6583×10^{-8}	0.995
1.8	1.7695	-1.3993×10^{-3}	6.0612×10^{-8}		0.999
	1.7695	-1.3880×10^{-3}	-3.2590×10^{-7}	2.8699×10^{-9}	0.999
2.7	1.7654	1.3609×10^{-3}	1.1982×10^{-7}		0.999
	1.7653	-1.4559×10^{-3}	3.3753×10^{-6}	-2.4172×10^{-8}	0.999
3.6	1.7551	-1.2904×10^{-3}	-1.2971×10^{-7}		0.999
	1.7551	-1.2741×10^{-3}	-6.8561×10^{-7}	4.1177×10^{-9}	0.999
4.5	1.7575	-1.2885×10^{-3}	-6.4636×10^{-8}		0.999
	1.7575	-1.3010×10^{-3}	3.6010×10^{-7}	-3.1462×10^{-9}	0.999

[a] Range: independent variable, $-10 < T < 100$ °C; experimental variable, $0 < X_{LiCl} < 4.5$ M. Units: g cm^{-3}.

(dynamic) viscosity, η, is more readily measured (*8*).

***Experimental Procedure*.** Capillary flow viscometers are almost exclusively used for the determination of viscosity coefficients in electrolytes. In principle, the time, t (seconds), required for a given volume of liquid, V (cm^3), to flow through a capillary of length l (centimeters) and radius r (centimeters) is measured. The absolute viscosity, η (centipoise), is computed by using the Poiseuille equation, eq 3, where $hg\rho$ is the applied

$$\eta = r^4\pi(hg\rho)t/(8lV) \qquad (3)$$

pressure differential, h (centimeters) is the average height of the liquid in the capillary, g (cm/s^2) is the acceleration due to gravity, and ρ (g/cm^3) is the density. The use of eq 3 implies that the fluid is Newtonian (i.e., η = constant, ρ = constant), the flow is laminar (i.e., the Reynolds number $N_{Re} < 2000$), and the fluid wall velocity is zero. To minimize kinetic energy corrections, capillary viscometers are designed to operate at $N_{Re} \simeq 300$ and flow times of less than 200 s.

Viscosities were measured by using the Cannon-Ubbelohde dilution viscometer immersed in mineral oil which was placed

J. Chem. Eng. Data **1983**, *28*, 52-56

in a drybox. The viscometer constant, **C** = $(hrg\rho)/2lV$, was determined by using viscosity standards provided by the Cannon Instrument Co. (*9*). To assure acceptable accuracy, the bath temperature was controlled to within ±0.01 °C and the time to within ±0.1 s.

Results. Kinematic viscosities of $SOCl_2$-based electrolytes were determined as a function of LiCl concentration (X_{LiCl}, M) and temperature (T, °C). Results are summarized in Tables VIII-XIII.

Densities

The density of any substance is the measure of the weight to volume ratio. A number of methods were devised to measure the density of liquids (*8*). Among them are pycnometric methods, dilatometers, hydrostatic balance, magnetic float, and buoyancy technique.

Experimental Procedure. The densities of the $SOCl_2$-based electrolytes were determined in Pyrex dilatometers whose volumes have been calibrated with methanol and distilled water. The accuracy within ±0.0001 g cm^{-3} is routinely obtained.

Results. Densities of $SOCl_2$-based electrolytes were determined as a function of LiCl concentration and temperature. Results are summarized in Tables XIV-XVIII.

Acknowledgment

We thank Mr. Maurice Murphy (NAVSEA 63R-32) and Dr. R. Lazar, Naval Underwater Systems Center, Rhode Island, Code 36301, for their interest and support.

Literature Cited

(1) Auburn, J. J.; French, K. W.; Lieberman, S. I.; Shah, V. K.; Heller, A. *J. Electrochem. Soc.* **1973**, *120*, 1613.

(2) Dey, A. N.; "Primary Li/$SOCl_2$ Cells XI: Performance and Safety of Super High Rate Li/$SOCl_2$ Batteries", 12th International Power Source Symposium, Brighton, 1980.

(3) Driscoll, J. R.; Szpak, S. *Proc.—Power Sources Symp.* **1982**, in press.

(4) Jones, G.; Bradshah, B. C. *J. Am. Chem. Soc.* **1933**, *55*, 1780.

(5) Washburn, E. W. *J. Am. Chem. Soc.* **1916**, *38*, 2431.

(6) Robinson, R. A.; Stokes, R. H. "Electrolyte Solutions", 2nd ed.; Academic Press: New York, 1959.

(7) Venkatasetty, H. V. *J. Electrochem. Soc.* **1975**, *122*, 245.

(8) Johnson, J. F.; Martin, J. R.; Porter, R. S. In "Techniques of Chemistry"; Weissberger, A., Rossiter, B. W., Eds.; Wiley: New York, 1977; Vol. I, Part VI.

(9) Cannon Instrument Co., State College, PA, Bulletin, No. 90.

Received for review February 22, 1982. Revised manuscript received July 21, 1982. Accepted August 9, 1982. This work was funded by Naval Sea Systems Command (NAVSEA 63R-32) through a propulsion block program and constitutes a fraction of a major program to establish a technology base for high rate discharge Li/$SOCl_2$ batteries.

Vapor-Liquid Equilibria for the Carbon Dioxide-1-Butene System at 37.7 and 45.0 °C

Paul K. Behrens[†] **and Stanley I. Sandler***

Department of Chemical Engineering, University of Delaware, Newark, Delaware 19711

A new high-pressure vapor-liquid equilibrium cell is described. Data taken with this cell for the CO_2-*n*-butane system at 37.7 °C are found to be in good agreement with those previously reported for this mixture. Data are also reported for the CO_2-1-butene system at 37.7 and 45.0 °C. All three sets of data were found to be correlated equally well by the Peng-Robinson, Soave-Redlich-Kwong, and Teja-Patel equations of state. Binary interaction parameters obtained by correlating our data are reported for each of these equations, and estimates of the critical points of CO_2-*n*-butane and CO_2-1-butene mixtures are given.

Introduction

Present interest in tertiary oil recovery by carbon dioxide flooding and synthetic fuels processing has encouraged us to initiate an experimental research program on the vapor-liquid equilibrium of carbon dioxide-hydrocarbon systems. Here we report the first results of this program which include the construction of a high-pressure vapor-liquid cell, the testing of our equipment by measuring vapor-liquid equilibrium data for a system (CO_2-*n*-butane) for which data have been published by others (*1*), and data for the CO_2-1-butene mixture over a range of conditions which have not been previously available (*2*). We also report on the fitting of our data with three different equations of state, and the estimation of mixture critical points for the systems studied.

Equipment

The heart of our equipment is a stirred, vapor and liquid recirculation equilibrium cell, shown in Figure 1. The cell is a large (1 L) autoclave manufactured by Autoclave Engineers, Inc., with a Magnedrive magnetically coupled stirrer driven by an external motor. To ensure the rapid attainment of vapor-liquid equilibrium, both the vapor and liquid phases are recirculated by using magnetically driven double-acting pumps constructed by us.

These pumps, shown in detail in Figure 2, consist of a barrel and heads constructed of nonmagnetic 316 stainless steel and a piston of magnetic 410 stainless steel. The piston, shown in Figure 3, has two Teflon rings and is driven by two electromagnet coils wrapped on the barrel of the pump. The magnetic field generated by the coil passes through the 316 stainless-steel barrel, to force the piston up or down depending on the coil being energized. A solid-state timer/power supply which we built pulses the coils in partially overlapping cycles so that the piston is decelerated near the end of its stroke. This provides pumping action while minimizing the piston-pump head contact at the end of each stroke. As indicated in Figures 2 and 3, four gravity-operated check values ensure the unidirectional flow of the pumped fluid with this dual-acting pump. Circulation of the phases using these pumps is confirmed in two ways. First, when the cell head is removed, the circulation of both phases is visually observed (indeed, this procedure is used to determine the optimum piston ring clearance). Second,

---

[†] Present address: Amoco Chemicals Corp., Amoco Research Center, Naperville, IL 60566.

0021-9568/83/1728-0052$01.50/0